

# Copula Models of Correlation: A DRAM Case Study

C. Glenn Shirley and W. Robert Daasch  
Integrated Circuits Design and Test Laboratory,  
Portland State University, Portland, Oregon, U.S.A

## Abstract<sup>1</sup>

*Variable bit retention time observed in a 65 nm DRAM case study will cause miscorrelation between retention times occurring in Test and Use. Conventional multivariate normal statistics cannot adequately model this miscorrelation. A more general copula-based modeling approach, widely used in financial and actuarial modeling, solves this problem. The DRAM case study shows by example how to use copula models in test applications. The method includes acquiring data using a test vehicle, fitting the data to a copula-based statistical model and then using the model to compute producer- and customer-oriented figures of merit of a product, different from the test vehicle. Different array size, fault tolerance schemes, test coverage, end-use (datasheet), and test condition specifications of the product are modeled.*

## 1. Introduction

Each bit of a dynamic random access memory (DRAM) retains its information as stored charge on a capacitor. After the bit has been written to, the charge leaks away so that valid data has a characteristic retention time. To retain the information, the bit must be read and refreshed with a specified time interval between refreshes. DRAM memory cells in every technology node can have a defect which causes a some bits to have a variable retention time (VRT), while most bits have stable retention times (SRT) [1][2][3]. The VRT behavior is an example of random telegraph noise (RTN) in gate-induced leakage (GIDL) current caused by a trap in gate oxide [4] or a defect in silicon [5] at the near-surface drain-gate boundary of the transistor in the DRAM cell. At any time the defect can transition reversibly between two states. One of the states is associated with a higher leakage current and shorter retention time.  $t_{\max}$  and  $t_{\min}$  are time constants of exponential distributions of duration of the maximum and minimum dwell times of a bit in the maximum and minimum retention time states. The states are maintained for many minutes [5], so retention times are manifested at the test process step in manufacturing (“Test”) differently from how they are manifested in end-use (“Use”). Test, being brief, may “see” a VRT bit in either the high or low leakage state. The probability that Test will find a bit in the maximum retention time state is  $s = t_{\max} / (t_{\max} + t_{\min})$ . On the other hand, since Use has an indefinite duration, a VRT bit’s high leakage state (worst-case) will certainly

occur in Use. If a VRT bit passes a Test screen in a low-leakage state, and the high leakage state causes the retention time in Use to be shorter than the specified refresh time, then the VRT bit will fail in Use.

The proportion of VRT bits can be controlled in the silicon fabrication process by reducing the density or passivating RTN-inducing defect, or by reducing the mechanical stress which activates the defect [6]. But Test screens and fault-tolerant array design are still needed to meet yield and quality targets for a product array of bits. Data with VRT bits which fail in Use are not suited to correction by ECC schemes used for soft errors (for example, due to cosmic rays) because of the performance impact of repeated error correction of a bit stuck in a failing state for many minutes. Run-time-repair schemes suited to “hard” bit failures [7] can be used.

The performance and quality requirements of a memory product may be met in different ways with possibly different costs. For example, the fraction of arrays with VRT bits escaping to Use, and failing, can be reduced by setting the Test retention time much longer than the refresh time in Use. This has a high cost of rejecting many good arrays (overkill) or repairing many “innocent” bits at Test. On the other hand, if a run-time-repair scheme is employed, the Test condition may be set closer to the Use condition and overkill may be reduced at the cost of design complexity. Tradeoffs like this occur at all stages of the product lifecycle, from product definition to manufacturing. Decision-making requires a statistical model of the memory product which adds considerations of array size, array repair capacity, Test conditions and datasheet (Use) specifications to the bit-level instability characteristics measured in recent studies [8]. This paper describes a new approach to the statistical modeling.

The paper breaks new ground in two aspects of statistical modeling: 1) Model-fitting involves selection of the mathematical forms of distributions to be used, and determination of goodness-of-fit of data to the models. 2) Inference involves “what-if” transformation of the fitted mathematical models to conditions different from the data (different array sizes, fault tolerance, different Test and Use conditions), and definition of the rules of decision-making. Decision-making rules use carefully-defined figures of merit closely related to cost models, such as yield loss (*YL*), overkill loss (*OL*), and customer-perceived defect level (*DL*).

---

<sup>1</sup> April 2013.

Model-fitting for semiconductor products usually involves fitting a multivariate normal (Gaussian) distribution to the data. But when a bivariate normal model was fitted to DRAM bit retention time data acquired at PSU’s ICDT lab (in Section 2.2 below) it was found that the model did not properly characterize the deep tail of the data. Unlike the data, the correlation in the Gaussian model fades away as one moves deeper into the bivariate tail. Actuarial and financial applications have also encountered this problem [9]. Inadequacy of multivariate normal models for financial and actuarial applications has motivated rapid development over the past decade of copula-based modeling methods because copulas provide a completely general approach to modeling multivariate dependency<sup>2</sup>. Nelsen [10], and Trivedi and Zimmer [11] give good introductions to copulas. This study finds that the Clayton copula, which differs fundamentally from the usual bivariate normal Gaussian model, is needed to describe the underlying dependency (correlation) structure of DRAM VRT behavior, and the way it is manifested in Test and in Use.

Statistical inference based on copula models has been developed for financial, actuarial and other applications, but not for semiconductor product applications. Semiconductor product applications require unique methods to handle scaling to various array sizes, for handling fault tolerance, for modeling Test and Use conditions, and for computing and using figures of merit closely related to product cost and quality models. This paper develops the necessary statistical machinery to do all of this for the DRAM application. The methods are, however, quite general and may be applied to any semiconductor product for which miscorrelation between Test and Use or among Test operations needs to be modeled.

The plan of the paper is as follows: In Section 3 copula models are extracted from the DRAM data described in Section 2. The central problem of model extraction is choice of the copula used to fit the data. Section 3 shows the shortcomings of the Gaussian copula, which mirrors the problem of multivariate normal models, and uses the “Clayton” copula which is well-suited to the DRAM data. Section 4 covers the inferential aspects of the application of copulas to test. These include:

- Modeling how Test and Use are manifested.
- Scaling from bit-level to array level.
- Modeling single bit fault tolerance.
- Modeling active repair at test.
- Definition of figures of merit (FOMs).

---

<sup>2</sup> In the statistical literature “dependency” is a more general term than “correlation”. Here the terms will be used interchangeably.

Section 5 describes where statistical copula-based modeling method fits in a wider context, and Section 6 indicates future directions.

## 2. DRAM Case Study

### 2.1. Experimental Design

The experiment follows a design similar in principle to that of Kim et. al [8] except that only the retention time minimum and maximum for each bit was determined. The experiment did not determine the time constants  $t_{\max}$  and  $t_{\min}$  of the maximum and minimum retention time states.

Test chips with four identical DRAM arrays on each chip were fabricated in a 65 nm process. Each of the four arrays on a test chip has 1,218,750 bits. Test chips were packaged in ball grid array packages and 10 test chips, prescreened for gross failures, were selected for the experiment.

The arrays were tested in PSU’s ICDT Lab on a Credence Quartet tester with temperature controlled by a Silicon Thermal Powercool LB300-i controller. Temperature was measured by a calibrated sensor on the silicon die. Pass/fail at 12 retention times for each bit in the array was determined at 18 environmental conditions, and the physical  $x,y$  location and retention time of each failing bit in the array was recorded. The environmental conditions were:

- Three temperatures: 105 °C, 115 °C, 125 °C.
- Three values of supply voltage,  $V_d$ : 0.8, 1.0, 1.2 volts.
- Two values of substrate bias,  $V_p$ : 0.4, 0.45 volts.

For each bit, 60 retention times in five groups of 12 were measured as follows:

- 12 retention times,  $r$ , were tested, increasing from 60 au to 604 au in steps of 49.5 au:  $r = 10 + i \times 49.5$  au,  $i = 1$  to 12, with pass/fail determined at each test stop,  $i$ . Retention times are given in arbitrary units (au), related to the true retention times by a numerical ratio.
- Each group of 12 retention times was repeated five times. Groups were separated by variable durations, typically many hours.

Figure 1 shows how the maximum observed retention time index  $i_{\max}$  and the minimum observed retention time index  $i_{\min}$  were extracted from the pass/fail pattern. If  $i_{\max} - i_{\min} \geq 2$  the bit is classified as VRT, otherwise it is SRT. A difference of 2 eliminates tester quantization effects which might misclassify SRT bits as VRT bits, at the risk of classifying some less variable VRT bits as SRT bits. If the leftmost retention time index in any group is 1 (fail) the bit is “dead” and is excluded from the study.

```

Group 1: 000110111111
Group 2: 000001111111
Group 3: 000111101111
Group 4: 000001111111
Group 5: 000111111111
          ↓ First zero from right.
AND: 000000101111  $i_{max} = 8$ 
OR:  000111111111  $i_{min} = 3$ 
          ↑ Last zero from left.

```

Figure 1. Example of the pass/fail pattern of a VRT bit and extraction of  $i_{max}$  and  $i_{min}$ . Pass/Fail is indicated by 0/1.

## 2.2. Experimental Results

Table I summarizes failing bit counts sampled from 49 Mb across all environmental conditions. Six bits were found to be dead and were excluded from analysis. At each environmental condition “live” bits passing at least the first test stop and with  $r < 604$  au are classified as SRT or VRT. A given bit may be classified differently in different environmental conditions. For example, 1610 failing bits showed only SRT behavior, and 288 bits showed SRT behavior in at least one environmental condition and VRT behavior in at least one environmental condition. The total number of bits with  $r < 604$  au observed to fail in the sample of 48,750,000 bits (minus 6 dead bits) was  $A+B+C = 1962$ .

Table I Categories of bits with retention times  $\leq 604$  au failing in at least one of the 18 environmental conditions.

SRT-only	SRT, but not VRT	A	1610
VRT	VRT and SRT	B	288
	VRT, but not SRT	C	64
Total bits		N	48750000
SRT PPM		A/N	33
VRT PPM		(B+C)/N	7

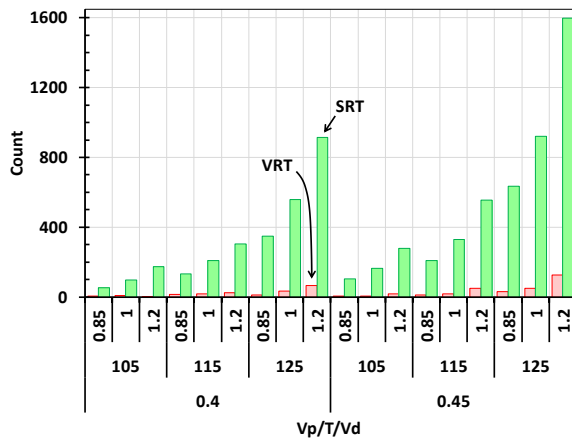


Figure 2. VRT and SRT counts vs. environmental condition sampled from  $10 \times 4 \times 1,218,750 = 48,750,000$  bits.

Figure 2 shows bit categories by environmental condition and Figure 3 gives a spatial map of the  $xy$  location of failing bits. Important observations are

- At the highest stress, retention times  $< 604$  au were observed for only a small fraction (40 PPM) of the population of bits. At less stressful environmental conditions, the fraction is smaller. These bits are representative of the “tail distribution” of retention times observed by White et al [12].
- Yield loss for a 1 Mb array with 1.2 PPM of bits defective, corresponding to the lowest environmental condition in the experiment, is 72%. Since array sizes of 1Mb and larger are generally used in applications, this shows that fault tolerance is required for any product array.
- 18% of the bits with  $r < 604$  au,  $(B+C)/(A+B+C)$ , show VRT behavior. This shows that VRT behavior must be included in any statistical model of DRAM retention time.
- Statistical analysis of the spatial distribution of failing bits in Figure 3 shows no evidence of clustering. The distribution of bit failures from die to die and array-to-array within dies is also indistinguishable from random. So the experiment may be regarded as sampling  $10 \times 4 \times 1218750 = 48,750,000$  (49 Mb) individual bits.

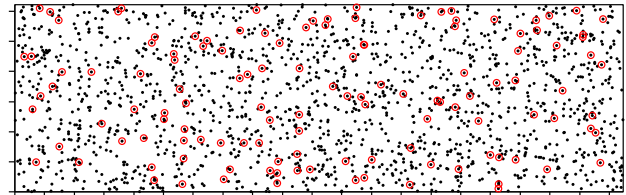


Figure 3 Map of spatial  $xy$  locations of all bits with  $r < 604$  au from 4 arrays on 10 chips, sampling 49 Mb. VRT bits are circled in red.

Each failing bit has a minimum and a maximum retention time. For stable bits, these retention times are equal. The fraction of time that an unstable bit is in the maximum versus minimum retention time state could not be empirically determined because the DRAM arrays in the test chips were indirectly accessed through a BIST controller which gives only pass/fail for a given refresh time. So, to construct a model of Test/Use correlation from the data it is necessary to additionally specify how retention time is manifested in Test and in Use. The manifestation will be different in Test and Use because in Use a given bit will be accessed an indefinite number of times and the minimum retention time will almost certainly occur, whereas Test is a single brief measurement for which the maximum or minimum retention time occurs with probability depending on the fraction of time-in-state.

Model-fitting is simplified by displaying the retention time data in a way that is different from any plausible Test/Use model with the understanding that, for decision-making, the data or fitted model will be transformed later into a plausible Test/Use model. The data display in Table II is

constructed by assigning  $(r_{\max}, r_{\min})$  to  $(r_1, r_2)$  or  $(r_2, r_1)$  with equal probability. Similar tables were generated for the 17 other environmental conditions. Several observations can be made: 1) The display of  $r_1$  and  $r_2$  in Table II does not represent a plausible Test/Use scenario of sequentially observed retention times because it does not include the possibilities of  $(r_1, r_2) = (r_{\min}, r_{\min})$  and  $(r_1, r_2) = (r_{\max}, r_{\max})$ . 2) Fitting a model to the data in Table

II is greatly simplified because only exchangeable copulas (symmetrical about  $r_1 = r_2$ ) and a single marginal distribution (the same for  $r_1$  and  $r_2$ ) need to be fitted due to symmetry of the data. 3) The data in Table II and any model fitted to it will be transformed later into a plausible Test/Use model via Eq. (14) and (15).

**Table II Maximum and minimum retention times at the highest environmental condition (rightmost bars in Figure 2) binned into cells using a “symmetrical” method of displaying the data.**

F = Cum N/SS (PPM)		r <sub>2</sub>			T = 125 C V <sub>p</sub> = 0.45 V V <sub>d</sub> = 1.2 V SS = 48,750,000													r (au)	
		Cum N	N	r (au)	604	0	0	0	0	1	0	1	1	1	1	18	69		
33.6	1639	273	555	0	0	0	0	0	0	0	0	0	0	1	14	104	95	59	
28.0	1366	343	505	0	0	1	0	0	0	0	1	2	10	97	92	120	20	20	
21.0	1023	237	456	0	0	0	0	0	0	0	1	5	46	83	86	14	2	2	
16.1	786	211	406	0	0	0	0	0	0	1	4	59	80	56	6	2	3	3	
11.8	575	156	357	0	0	0	0	0	0	1	29	68	53	2	1	2	0	0	
8.6	419	134	307	0	0	0	0	0	0	36	56	38	2	1	1	0	0	0	
5.8	285	109	258	0	0	0	0	15	71	20	2	1	0	0	0	0	0	0	
3.6	176	69	208	0	0	0	12	38	18	0	0	0	0	1	0	0	0	0	
2.2	107	61	159	0	0	8	43	9	0	0	0	0	0	0	0	0	0	1	
0.9	46	27	109	0	1	19	6	0	0	0	0	0	1	0	0	0	0	0	
0.4	19	13	60	0	11	2	0	0	0	0	0	0	0	0	0	0	0	0	
0.1	6	6	0	5	1	0	0	0	0	0	0	0	0	0	0	0	0	0	
				0	60	109	159	208	258	307	357	406	456	505	555	604	r (au)		
				5	13	30	61	63	127	112	175	195	255	308	302	N		r <sub>1</sub>	
				5	18	48	109	172	299	411	586	781	1036	1344	1646	Cum N			
				0.1	0.4	1.0	2.2	3.5	6.1	8.4	12.0	16.0	21.3	27.6	33.8	F=Cum N/SS (PPM)			

The marginal empirical cumulative distributions ( $F$  as a function of  $r_1$  and  $r_2$ ) given in Table II were fitted to a single Weibull distribution following Lieneweg et al.[13] and White et al. [12] as shown in Figure 4. The slope and intercept of the fitted lines give the shape,  $\beta$ , and scale,  $\alpha$ , parameters of the Weibull distribution of retention time:

$$F(r) = 1 - \exp\left[-\left(\frac{r}{\alpha}\right)^\beta\right]. \quad (1)$$

Fits like Figure 4 were done for every environmental condition. The shape parameter  $\beta$  was always nearly 2, so the model was simplified by forcing  $\beta$  to 2.  $\beta=2$  results in a small under-estimate of the retention time at short retention times, which is conservative. Arrhenius temperature and exponential voltage dependence gave an excellent fit (Figure 5) to the scale parameters,  $\alpha$  for  $\beta=2$ , extracted from all environmental conditions:

$$\ln \alpha = \ln \alpha_0 + a(V_p - V_{p0}) + b(V_d - V_{d0}) + \frac{Q}{k_B} \left( \frac{1}{T} - \frac{1}{T_0} \right) \quad (2)$$

The good fit shown in Figure 5 means that the single parameter  $\ln \alpha$  computed from Eq. (2) may be used as a measure of the combined effect of  $V_d$ ,  $V_p$ , and  $T$ . This simplifies the display of the environmental dependencies observed in this study. The leftmost point in Figure 5 (smallest  $\alpha$ ) corresponds to Figure 4 and Table II. A practical benefit of the good fit is that a given value of  $\ln \alpha$  defines a surface (nearly a plane) of “equivalent test set points” in  $(V_p, V_d, T)$  space. This gives useful flexibility when integrating different kinds of test into a test program.

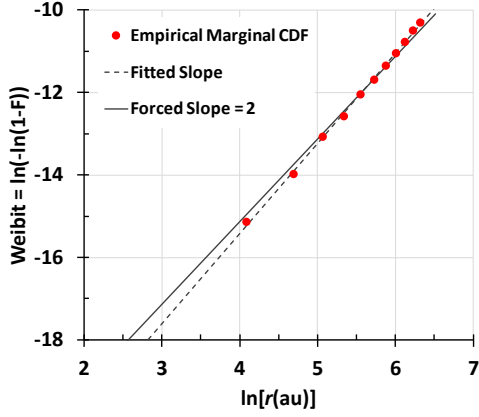


Figure 4. Weibull fit of marginal distributions at the highest environmental condition, from Table II.

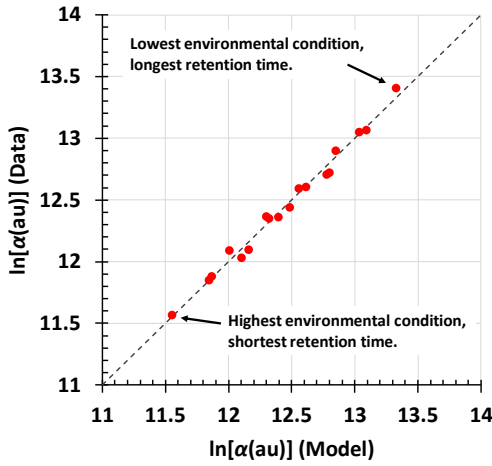


Figure 5. Extracted vs. model-fitted, Eq. (2), scale parameter  $\alpha$  for all 18 environmental conditions.

The distribution of data across  $r_1$  and  $r_2$  cells in Table II, and at 17 other environmental conditions was characterized by Kendall's tau. Suppose the retention times,  $r_1$  and  $r_2$ , are known exactly for each of  $n$  measured bits so that every bit may be ranked by  $r_1$  and by  $r_2$  without ties. The number of bit-pairs,  $n(n-1)/2$  comprises  $k$  "concordant" pairs and  $d$  "discordant" pairs. For a concordant pair, the relative ranks of  $r_1$  for a bit pair is the same as the relative ranks of  $r_2$  of the bit pair. For a discordant pair the relative ranks are different. Kendall's tau for the sample (indicated by the prime) is  $\tau' = (k - d)/(k + d)$ .

Test correlation data is typically binned into cells as in Table II so that Kendall's tau must be calculated for data with many ties. The definition of tau has been extended [14] to take ties into account. The sample tau for data with ties is

$$\tau' = \frac{k - d}{\sqrt{\frac{1}{2}n(n-1) - U} \sqrt{\frac{1}{2}n(n-1) - V}} \quad (3)$$

$$U = \frac{1}{2} \sum u(u-1), \quad V = \frac{1}{2} \sum v(v-1)$$

where any bit pairs that are tied in  $r_1$  or  $r_2$  are not counted in  $k$  or  $d$  and where, in  $U$ ,  $u$  is the number of tied  $r_1$  values in each set.  $V$  is defined in the same way, but for  $r_2$  values. Code to compute  $\tau'$  from data with ties is available in many statistical software packages. Sample taus for the data in Table II, and 17 other environmental conditions were computed by Eq. (3) and plotted in Figure 6. Also plotted in Figure 6 is the fraction of the population sampled at each environmental condition, ranging from 35 PPM at the highest stress (smallest  $\alpha$ ) to 1.2 PPM at the lowest stress. A remarkably constant value of  $\tau' = 0.828$ , independent of environmental condition, is observed. If only the diagonal cells in Table II were populated, the value of the sample tau would be unity.

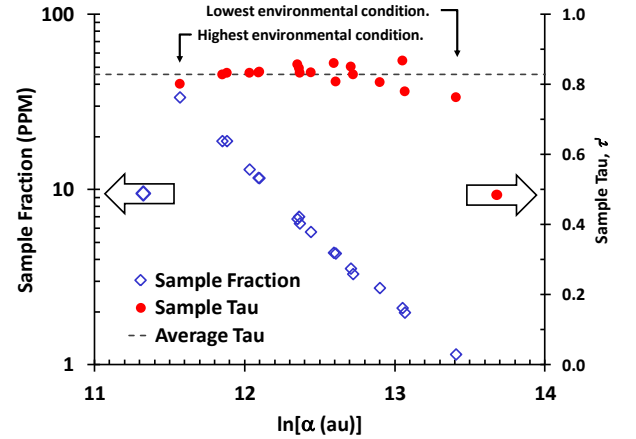


Figure 6. Sample tau is independent of sample fraction and environmental conditions ( $\ln \alpha$ ).

Extracted parameters of the marginal distribution model, Eq. (2), are given in Table III along with parameters describing the correlation (aka "Dependence") including copula parameters described in the following Section.

Table III Parameters of extracted marginal and dependence models for the symmetrical coverage model.

Margin	$\beta$	2.0
	$\ln[a_0 \text{ (au)}]$	11.57
	$a \text{ (V}^{-1}\text{)}$	-5.79
	$b \text{ (V}^{-1}\text{)}$	-1.55
	$Q \text{ (eV)}$	0.605
	$V_{p0} \text{ (V)}$	0.45
	$V_{d0} \text{ (V)}$	1.2
	$T_0 \text{ (}^\circ\text{C)}$	125.0
Dependence	Sample Tau, $\tau'$	0.828
	Clayton Copula, $\theta$	9.74
	Gaussian Copula $(1-\rho) \times 10^3$	0.695

### 3. Modeling Dependence Using Copulas

#### 3.1. Copula Background

If the cell-counts in Table II are divided by the sample size to give the probability mass in the cell, then the table is an empirical 2-dimensional probability density function (pdf) sampling a population pdf  $h(r_1, r_2)$ . The corresponding bivariate cumulative distribution function (cdf) is

$$H(r_1, r_2) = \int_0^{r_1} dx \int_0^{r_2} dy h(x, y). \quad (4)$$

For marginal distributions  $F(r_1) = H(r_1, \infty)$ , and  $G(r_2) = H(\infty, r_2)$  (in the present application  $F = G$ ), the definition of a copula  $C$  is given by  $H$  written as a function of the marginal distributions

$$H(r_1, r_2) = C[F(r_1), G(r_2)] \quad (5)$$

or

$$C(u, v) = H[F^{-1}(u), G^{-1}(v)]. \quad (6)$$

A two-dimensional copula is a function on the unit square domain with range  $[0, 1]$ , which:

- Is grounded.  $C(u, 0) = 0 = C(0, v)$ .
- Is normalized.  $C(1, 1) = 1$ .
- Has uniform marginal distributions.  
 $C(u, 1) = u$  and  $C(1, v) = v$ .
- Is 2-increasing, so that for every  $u_1, u_2, v_1, v_2$  in  $[0, 1]$  such that  $u_1 \leq u_2$  and  $v_1 \leq v_2$  the probability mass in the rectangular area defined by  $(u_1, v_1)$  and  $(u_2, v_2)$  is positive definite

$$C(u_2, v_2) - C(u_2, v_1) - C(u_1, v_2) + C(u_1, v_1) \geq 0.$$

The definitions have generalizations to more than two dimensions.

Sklar showed that for a given  $H$ , the copula  $C$  is unique. And Schweizer and Wolff showed that  $C$  is invariant under monotonic transformations of  $F$  and  $G$ . This history, and more, is covered by Nelsen [10]. These results are profound because they imply that  $C$  contains *all* of the rank-dependency information in *any* multivariate cdf, and that the study and modeling of this dependency can be completely decoupled from details of the marginal distributions.

Two copulas are especially important:

$$C(u, v) = \begin{cases} \min[u, v] & \text{Perfect correlation} \\ uv & \text{Independence} \end{cases} \quad (7)$$

Also important is the definition of tail dependency in the low tail

$$LT = \lim_{u \rightarrow 0^+} \frac{C(u, u)}{u}. \quad (8)$$

Notice that  $LT$  for perfect correlation is unity, whereas for independence  $LT$  vanishes.

Kendall's tau may be calculated analytically from a copula by

$$\tau = 4 \int_0^1 \int_0^1 C(u, v) \frac{\partial^2 C(u, v)}{\partial u \partial v} du dv - 1. \quad (9)$$

For perfect correlation  $\tau = 1$ , for perfect anti-correlation  $\tau = -1$ , and for independence  $\tau = 0$ . Eq. (9) can be generalized to compute  $\tau$  for truncated regions of the copula [15].

Copulas come in families spanned by adjustable parameters and Eqs. (8) and (9) provide a way to fit the model parameters to data. For example, if the empirical value of  $\tau$  is known from Eq. (3), then the value of the parameter of a single-parameter copula may be determined by comparison with the model  $\tau$  determined by an integral like Eq. (9) integrated over a truncated region of the copula corresponding to the data sample.

Copulas give a complete generalization of the usual multivariate normal approach for modeling statistical dependency. But this leads to the main problem of copula modeling; choosing the appropriate copula. The universe of possible functions even in two dimensions is vast, so some application-specific guidance is needed. In the course of this work several kinds of copula were tried for the DRAM; the Gaussian copula, geometrical copulas, various kinds of Archimedean copulas, the Marshall-Olkin copula, and convex combinations of various copulas [10]. Just two of the fitting attempts are described in the following; the Gaussian copula, and the Clayton copula (an Archimedean copula). The Gaussian copula is described because it is the conventional multivariate normal modeling approach in copula guise and therefore shows the problem with conventional multivariate normal modeling. The Clayton copula is shown because it is the best model found, and was used in subsequent application of the model.

#### 3.2. The Gaussian Copula

In two dimensions, the Gaussian copula is

$$C(u, v; \rho) = \frac{1}{2\pi\sqrt{1-\rho^2}} \int_{-\infty}^{\Phi^{-1}(u)} \int_{-\infty}^{\Phi^{-1}(v)} \exp\left[-\frac{x^2 - 2\rho xy + y^2}{2(1-\rho^2)}\right] dy dx \quad (10)$$

where  $\Phi$  is the standard normal distribution. Numerical methods to compute bi-variate and tri-variate integrals like Eq. (10) are available [16]. The Gaussian copula was

fitted to the data of Table II by finding  $\rho$  which minimizes the sum of squares:

$$SSQ(\rho) = \frac{\sum_i \sum_j (N \times \delta C_{ij}(\rho) - n_{ij})^2}{\sum_i \sum_j n_{ij}^2} \quad (11)$$

where  $i$  and  $j$  are cell indexes in Table II and

$$\delta C_{ij} = C_{ij} - C_{i-1,j} - C_{i,j-1} + C_{i-1,j-1}. \quad (12)$$

$\delta C_{ij}$  is the probability mass in cell  $ij$  with  $C_{ij}$  computed via Eq. (10) at each cell  $ij$ ,  $n_{ij}$  is the count in a cell, and  $N = 48,750,000$ . This was repeated for each of the 18 environmental conditions and the fitted values of  $1 - \rho$  were plotted vs environmental condition in Figure 7.

The value of  $\rho$  must be forced to within a few parts in 10,000 of unity to fit the observed data which are the deep tail (1.2 to 35 PPM) of the bit population. The tiny value of  $1 - \rho$  shows a key problem with multivariate normal modeling and with the Gaussian copula which has been recognized in other fields [9]. As one moves from the bulk of the population into the tails the correlation in the Gaussian copula fades away unless  $\rho$  is exactly unity. That is, for the Gaussian copula,  $LT = 0$  except when  $\rho \equiv 1$ . The Gaussian copula's tail dependency may be valid for intrinsic properties of devices, but for defect-related mechanisms such as the retention time mechanisms of the DRAM one would expect that dependency would be maintained no matter how far into the tail the sample is taken. That is, one would prefer a copula for which  $LT \neq 0$ . The significant scatter in  $1 - \rho$  as a function of environmental conditions in Figure 7 also shows that the Gaussian copula is not a "natural" fit to the data. The average of  $1 - \rho$  across environmental conditions is given in Table III above.

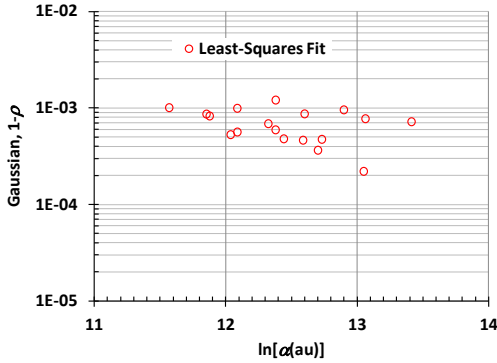


Figure 7. Values of  $1 - \rho$  for the Gaussian copula fitted by least squares to data like Table II, as a function of environmental condition.

### 3.3. The Clayton Copula

The Clayton copula (see [10], p118) for the range of  $\theta$  of interest is

$$C(u, v; \theta) = (u^{-\theta} + v^{-\theta} - 1)^{-1/\theta} \quad (0 < \theta < \infty) \quad (13)$$

where  $\theta \rightarrow 0$  corresponds to independence, and  $\theta \rightarrow \infty$  corresponds to perfect correlation. The probability density map corresponding to Eq. (13) for the parameter value  $\theta = 9.74$  which fits the DRAM data is reflected in the density of  $(u, v)$  points in Figure 8 synthesized by standard methods described in [11] (Appendix) and [17].

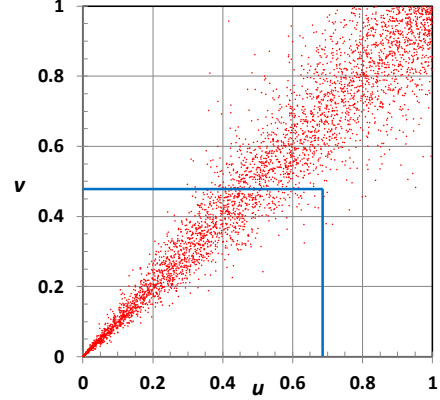
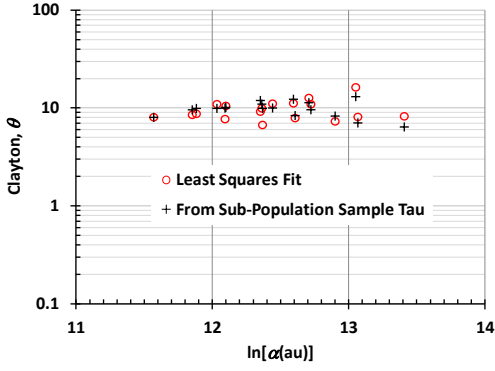


Figure 8. Probability density map for Clayton copula with  $\theta = 9.74$ , and example rectangular truncation.

Properties of the Clayton copula include the low-tail dependence,  $LT = 2^{-1/\theta}$  and Kendall's tau for the entire probability space,  $\tau = \theta/(\theta+2)$  derived using Eqs. (8) and (9), respectively, with Eq. (13). Recently Oakes [15] showed that the Clayton copula is the only absolutely continuous copula with a remarkable "truncation-invariance" property: If the probability map of any rectangular truncation of the copula with one corner pinned at  $(0,0)$  as shown in Figure 8 is re-mapped to the entire copula space,  $[0, 1]^2$ , then the same Clayton copula (same  $\theta$ ) is recovered. A consequence of this is that tau computed from any rectangular truncation of the probability density map with one corner pinned at  $(0,0)$  is always  $\theta/(\theta+2)$ .

Figure 6 shows that the Kendall's tau for the failing bits remains constant as a larger and larger sample of the 49 Mb population is exposed by increasing the test environmental condition (reducing  $\ln \alpha$ ). The samples correspond to square truncations of the empirical copula with one corner fixed at  $(0,0)$ , and the opposite corner at  $(x,x)$ , where  $x$  varies with the environmental condition. Tau for the Clayton copula is also invariant as data is truncated by rectangles (and, *a fortiori*, squares) like the one shown in Figure 8. So the Clayton copula is a plausible model for the observed dependency behavior. Occam's razor was used to choose the Clayton copula over others with small but non-vanishing truncation variation of  $\tau$ . Figure 9 shows  $\theta$  for the Clayton copula fitted at each of the 18 environmental conditions the same least squares method used for the Gaussian copula. Figure 9 also shows  $\theta$  determined from Figure 6 using the inverse of the relation between  $\tau$  and  $\theta$  for the Clayton copula:  $\theta = 2\tau/(1 - \tau)$ .



**Figure 9. Values of  $\theta$  vs environmental condition ( $\ln \alpha$ ) for the Clayton copula fitted by least squares to data like Table II, and by  $\theta = 2\tau/(1 - \tau)$  from  $\tau$  in Figure 6.**

Monte-Carlo synthesis of random vectors  $(u_i, v_i)$  from a copula is often needed to “play back” a model to validate it, or to do numerical calculations when analytical calculations are intractable. The Clayton copula has a very useful property for Monte-Carlo simulation stemming from the truncation invariance. It is possible to synthesize points in a truncated region of the copula shown in Figure 8 *without rejection*. This feature of the Clayton copula and of certain other copulas is very important for efficient simulation because only the extreme tail of the distribution (40 PPM in the current example – a tiny area near the origin in Figure 8) is of practical interest and needs to be synthesized. The Gaussian copula does *not* have this feature and requires extensive rejection to generate tail samples. This is another significant disadvantage of the conventional multivariate normal approach.

## 4. Application

### 4.1. Model of Test and Use

The symmetrically displayed bit data in Table II were fitted to an exchangeable copula (symmetrical in its arguments,  $C(u, v) = C(v, u)$ ). Although the fitted exchangeable copula is not a plausible model of Test and Use, the exchangeable copula may be transformed into a pseudo-copula (having properties of a copula except for non-uniform margins) which is a plausible model of the way Test and Use are manifested. An advantage of this approach is that different Test/Use scenarios may be explored by varying the transformation of the fitted copula.

A plausible model of Test and Use manifestation is one in which the maximum retention time of a given bit is exhibited at Test with probability  $s = t_{\max}/(t_{\max} + t_{\min})$  (and minimum retention time is exhibited at Test with probability  $1 - s$ ) while the minimum retention time for the bit is *always* exhibited in Use. If  $r_1$  and  $r_2$  are retention times sampled from the symmetrically displayed data of Table II or sampled by Monte-Carlo from the

fitted symmetrical model (the Clayton copula) then the plausible Test/Use model is

$$r_{Use} = \min[r_1, r_2] = r_{\min} \quad \text{All the time.}$$

$$r_{Test} = \begin{cases} \max[r_1, r_2] = r_{\max} & \text{Proportion } s \text{ of the time.} \\ \min[r_1, r_2] = r_{\min} & \text{Proportion } 1 - s \text{ of the time.} \end{cases} \quad (14)$$

The probability density map obtained by using Eq. (14) with  $s = 0.8$  to transform the symmetrical model Clayton copula density map in Figure 8 is shown in Figure 10.

Association of minimum retention time of a bit with Use is realistic because a bit will be accessed an indefinite number of times making it certain the minimum retention time will occur eventually. Test, however is a single brief event so association of the maximum or minimum retention time with Test depends on the probability,  $s$ , that the bit happens to be in the maximum retention time state when tested. The assumption that the bit is *always* in the maximum retention time state at Test ( $s = 1$ ) is conservative from the customer perspective because a model based on this will over-estimate DPPM in Use, and thereby lead to customer-conservative Test and Use specifications.

Using methods of Nelsen (problem 2.16 on p26 of [10]), and Navarro and Spizzichino [18], it can be shown that since the marginal distributions for  $r_1$  and  $r_2$  are the same in the symmetrical model by construction, the transformation of Eq. (14) may be written as a transformation of the fitted exchangeable copula  $C$  into the pseudo-copula  $D$ :

$$D(u, v) = s[C(u, v) + C(v, z) - C(u, z)] + (1 - s)[2z - C(z, z)] \quad (15)$$

$$z = \min[u, v]$$

Figure 10 shows the density map of  $D$  when  $C$  is the Clayton copula with  $\theta = 9.74$  and  $s = 0.8$ .

### 4.2. Test Set Points and Datasheet Specifications

Test set points and datasheet specifications (Use conditions) are expressed in terms of environmental conditions ( $V_p, V_d, T$ ) and retention time,  $r$ . These four parameters at Test and at Use are usually set so that the Test set point is more “stressful” (causes more failures) than the Use condition. The environmental conditions ( $V_p, V_d, T$ ) are mapped into  $\alpha_{Test}$  in Test and  $\alpha_{Use}$  in Use by Eq. (2). So a single parameter,  $u$ , depending on both the environmental condition via  $\alpha_{Use}$  and retention time limit  $r_{Use}$  in the datasheet defines the datasheet specification (Use condition), and a single parameter,  $v$ , defines the Test set point:

$$u = 1 - \exp\left[-\left(\frac{r_{Use}}{\alpha_{Use}}\right)^\beta\right] \quad v = 1 - \exp\left[-\left(\frac{r_{Test}}{\alpha_{Test}}\right)^\beta\right]. \quad (16)$$



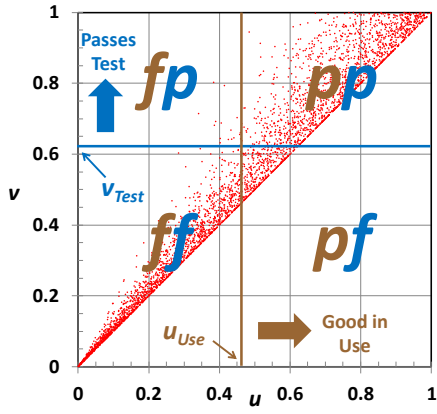


**Figure 10.** Test and Use conditions divide the bit pseudo-copula  $D$  (with  $\theta = 9.74$ ,  $s = 0.8$ ) into four categories labeled by  $fp$ ,  $pf$ ,  $ff$ ,  $pp$ , where the first character refers to Use and the second to Test.

When the Test set point and datasheet specifications  $u$  and  $v$  are superimposed on the bit pseudo-copula,  $D$ , as in Figure 10, the probability masses associated with each of the four regions are given by

$$\begin{aligned} p_{fp} &= D(u,1) - D(u,v) & p_{pf} &= D(1,v) - D(u,v) \\ p_{ff} &= D(u,v) & p_{pp} &= 1 - p_{fp} - p_{pf} - p_{ff} \end{aligned} \quad (17)$$

where, for example,  $p_{fp}$  is the fraction of bits failing in Use and passing in Test.

### 4.3. Array Statistics and Fault Tolerance

The random spatial distribution of bit failures (Figure 3), the large sample size of bits (49 Mb), and the small probability of failure (1 to 40 PPM, depending on environmental condition) easily justifies use of the Poisson approximation to model the statistics of arrays of bits. Consider an array of  $n$  bits. The probability that the array has exactly  $n_{fp}$ ,  $n_{pf}$ , and  $n_{ff}$  bits in the mutually exclusive categories defined in Figure 10 is

$$\begin{aligned} P(N_{fp} = n_{fp}, N_{pf} = n_{pf}, N_{ff} = n_{ff}) \\ = \frac{\lambda_{fp}^{n_{fp}} \exp(-\lambda_{fp})}{n_{fp}!} \frac{\lambda_{pf}^{n_{pf}} \exp(-\lambda_{pf})}{n_{pf}!} \frac{\lambda_{ff}^{n_{ff}} \exp(-\lambda_{ff})}{n_{ff}!} \end{aligned} \quad (18)$$

where

$$\lambda_{fp} = np_{fp}, \quad \lambda_{pf} = np_{pf}, \quad \lambda_{ff} = np_{ff}. \quad (19)$$

Fault tolerance is modeled by expanding the definition of a “good” array to include arrays with some “bad” bits. Bad bits in arrays that are considered good are taken to be covered by a fault tolerance scheme. The maximum number of bad bits which can be tolerated is a measure of the capacity of the fault tolerance scheme. Suppose an array can tolerate up to  $n_t$  bits bad in Test and up to  $n_u$  bits bad in Use. Also suppose that the bits tolerated in Test are not repaired, but are included in the bad bits tolerated in Use. Then the probability that the array “Passes Test”

is the sum of Eq. (18) over sets of integers  $n_{fp}$ ,  $n_{pf}$  and  $n_{ff}$  allowed by the constraint  $n_{ff} + n_{pf} \leq n_t$  ( $n_{fp}$  is unconstrained). And the probability the array is “Good in Use” is a sum constrained by  $n_{ff} + n_{fp} \leq n_u$  ( $n_{pf}$  is unconstrained). The probability that an array “Passes Test and is Good in Use” is a sum over values of  $n_{fp}$ ,  $n_{pf}$  and  $n_{ff}$  which satisfy both  $n_{ff} + n_{pf} \leq n_t$  and  $n_{ff} + n_{fp} \leq n_u$ . A geometrical interpretation of the regions of bit category index space corresponding to three array categories is shown in Figure 11.

Analytical expressions for the sums over terms like Eq. (18) corresponding to the zones in Figure 11 are expressible in terms of the bi-variate correlated Poisson distribution introduced by Campbell [19], derived as follows: If an array has exactly  $n_u$  bits which are bad in Use and exactly  $n_t$  bits which are bad at Test, then  $n_{fp}$ ,  $n_{pf}$  and  $n_{ff}$  may vary within the following constraints:

$$n_u = n_{ff} + n_{fp} \quad n_t = n_{ff} + n_{pf} \quad 0 \leq n_{ff} \leq \min[n_u, n_t] \quad (20)$$

where the last inequality is a way of expressing the constraints  $n_{pf} \geq 0$  and  $n_{fp} \geq 0$ .

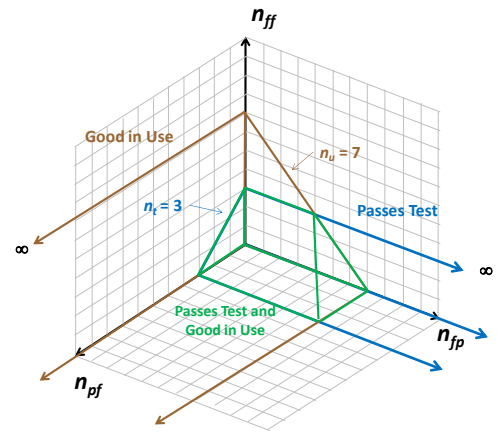


**Figure 11.** Zones of bit category space corresponding to three array category probabilities for bad bits tolerated *but not repaired* at Test, and tolerated in Use. For  $n_u = 7$  and  $n_t = 3$ .

So if  $N_u$  and  $N_t$  are random variables giving the number of failing bits in Use and Test respectively, the probability that an array has *exactly*  $n_u$  bits failing in Use and *exactly*  $n_t$  bits failing in Test is the sum of Eq. (18) over values of  $n_{ff}$  allowed by Eq. (20):

$$\begin{aligned} P(N_u = n_u, N_t = n_t) \\ = e^{-(\lambda_{fp} + \lambda_{pf} + \lambda_{ff})} \sum_{n_{ff}=0}^{\min[n_u, n_t]} \frac{\lambda_{fp}^{n_u - n_{ff}} \lambda_{pf}^{n_t - n_{ff}} \lambda_{ff}^{n_{ff}}}{(n_u - n_{ff})! (n_t - n_{ff})! n_{ff}!} \quad (21) \\ \equiv \text{pois}(n_u, n_t; \lambda_{fp}, \lambda_{pf}, \lambda_{ff}). \end{aligned}$$

The cumulative form of this distribution is

$$\begin{aligned}
P(N_u \leq n_u, N_t \leq n_t) &= \sum_{m=0}^{n_u} \sum_{n=0}^{n_t} \text{pois}(m, n; \lambda_{fp}, \lambda_{pf}, \lambda_{ff}) \\
&= \sum_{i=0}^{\min\{n_u, n_t\}} \frac{\lambda_{ff}^i e^{-\lambda_{ff}}}{i!} R(\lambda_{fp}, n_u - i) R(\lambda_{pf}, n_t - i) \\
&\equiv \text{Pois}(n_u, n_t; \lambda_{fp}, \lambda_{pf}, \lambda_{ff})
\end{aligned} \tag{22}$$

where  $R$  is the univariate cumulative Poisson distribution available in many software packages:

$$R(x, n) \equiv e^{-x} \sum_{0 \leq i \leq n} \frac{x^i}{i!} \tag{23}$$

which vanishes when  $n < 0$ .  $n_u$  and  $n_t$  are usually small integers so calculation of the cumulative bivariate Poisson distribution using the second equality in Eq. (22) is easy. Eqs. (21) and (22) are Campbell's [19] bivariate correlated Poisson distribution. Johnson, Kotz, and Balakrishnan [20] point out that Eq. (21) is the distribution of

$$N_u = N_{fp} + N_{ff} \quad N_t = N_{pf} + N_{ff} \tag{24}$$

where  $N_{fp}$ ,  $N_{pf}$ , and  $N_{ff}$  are mutually independent Poisson random variables with means  $\lambda_{fp}$ ,  $\lambda_{pf}$ , and  $\lambda_{ff}$ . On the margins (that is, with  $n_t = \infty$  or  $n_u = \infty$ ),  $N_u$  and  $N_t$  have Poisson distributions with means  $\lambda_{ff} + \lambda_{fp}$  and  $\lambda_{ff} + \lambda_{pf}$ , respectively.

The mapping of proportions of three Test/Use categories of *bits* into proportions of three Test/Use categories of *arrays* with specified fault tolerance is given by Campbell's correlated Poisson distribution, Eq. (22). If an array can tolerate up to  $n_u$  bad bits in Use and up to  $n_t$  bad bits in Test then the probability that the array "Passes Test and is Good in Use" corresponds to sums over bit category indexes in the intersection of the two infinite prisms along the  $n_{pf}$  and  $n_{fp}$  axes in Figure 11, and is

$$\begin{aligned}
P(\text{Passes Test and Good in Use}) &= \text{Pois}(n_u, n_t; \lambda_{fp}, \lambda_{pf}, \lambda_{ff}) \\
&= \text{Pois}(n_u, n_t; \lambda_{fp}, \lambda_{pf}, \lambda_{ff}).
\end{aligned} \tag{25}$$

The probability that the array tolerates  $n_u$  bits in Use, irrespective of the number of bad bits in Test the sum of Eq. (18) over bit category indexes in the prism running down the  $n_{pf}$  axis in Figure 11 and is

$$\begin{aligned}
P(\text{Good in Use}) &= \text{Pois}(n_u, n_t = \infty; \lambda_{fp}, \lambda_{pf}, \lambda_{ff}) \\
&= R(\lambda_{ff} + \lambda_{fp}, n_u).
\end{aligned} \tag{26}$$

The probability that the array tolerates  $n_t$  bits in Test, irrespective of the number of bad bits in Use corresponds to a sum of Eq. (18) over bit category indexes in the prism running down the  $n_{fp}$  axis in Figure 11 and is

$$\begin{aligned}
P(\text{Passes Test}) &= \text{Pois}(n_u = \infty, n_t; \lambda_{fp}, \lambda_{pf}, \lambda_{ff}) \\
&= R(\lambda_{ff} + \lambda_{pf}, n_t).
\end{aligned} \tag{27}$$

In practice these expressions would be applied when the fault tolerance mechanism on the chip is enabled in both Test and Use ( $n_t = n_u > 0$ ).

When the tester *actively repairs* the bits that it tolerates, the constraints on the integers  $n_{fp}$ ,  $n_{pf}$  and  $n_{ff}$  allowed in the sums over terms like Eq. (18) are changed from the constraints shown in Figure 11 to the constraints shown in Figure 12. Repair of bits tolerated at Test causes the tolerance mechanisms in Use to have fewer *ff* category bits to tolerate. So, more tolerance capacity is available in Use for test escape bits (*fp* category bits) and *ff* bits exceeding the repair capacity of Test. The effect is seen in Figure 12 as an extra volume of bit category index space on top of the "Good in Use" volume shown for the no-repair-at-Test case in Figure 11. As before, the "Passes Test and Good in Use" volume is the intersection of the "Good in Use" and the "Passes Test" volumes, so its probability sum changes too. The "Passes Test" volume is the same as for the no-repair-in-test case.

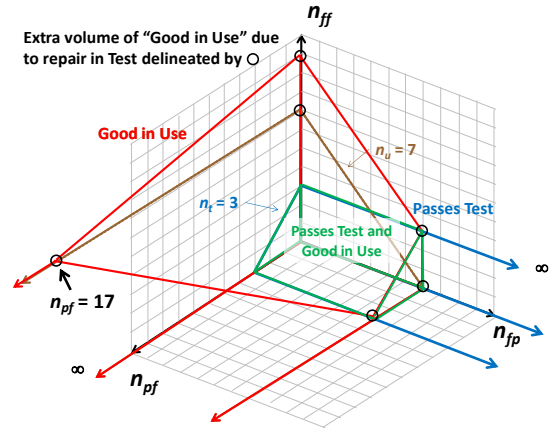


**Figure 12. Zones of bit category space corresponding to three array category probabilities for bad bits tolerated and repaired at Test, and tolerated in Use. For  $n_u = 7$  and  $n_t = 3$ .**

The probability expressions corresponding to the volumes in Figure 12 are

$$\begin{aligned}
P(\text{Good in Use}) &= L(\lambda_{ff}, \lambda_{fp}, \lambda_{pf}, n_u, n_t) \\
&\quad + R(\lambda_{ff} + \lambda_{fp}, n_u)
\end{aligned} \tag{28}$$

where  $L$  is the sum of terms like Eq. (18) over the "extra" volume of "Good-in-Use" bit category space in Figure 12.  $L$  does not have a tidy analytical expression, but it is easily evaluated because the the number of terms in the "extra" volume is finite and small. The "Passes Test and Good in Use" volume in Figure 12 is a simpler truncated prism than the corresponding shape in Figure 11, giving

$$\begin{aligned}
P(\text{Passes Test and Good in Use}) \\
= R(\lambda_{fp}, n_u) R(\lambda_{ff} + \lambda_{pf}, n_t). \quad (29)
\end{aligned}$$

Finally, the ‘‘Passes Test’’ probability for active repair is the same as Eq. (27) for no-repair-at-test, as it must be because this proportion will be agnostic to the repair status of Test-tolerated bits.

#### 4.4. Figures of Merit and Decision-Making

Manufacturing and quality figures of merit (FOMs) can be expressed in terms of the three array probabilities,  $P(\text{Passes Test})$ ,  $P(\text{Good in Use})$ , and  $P(\text{Passes Test and Good in Use})$  derived in Section 4.3. The FOMs are required to meet target values to determine fault tolerance, test specifications, and datasheet specifications of the product. The FOMs are yield loss ( $YL$ ), overkill loss ( $OL$ ), and end-use defect level ( $DL$ ).  $YL$  and  $OL$  are producer-oriented cost-related FOMs, and  $DL$  is a customer-oriented quality FOM. Figure 13 shows how these FOMs are related to the probabilities derived in Section 4.3.

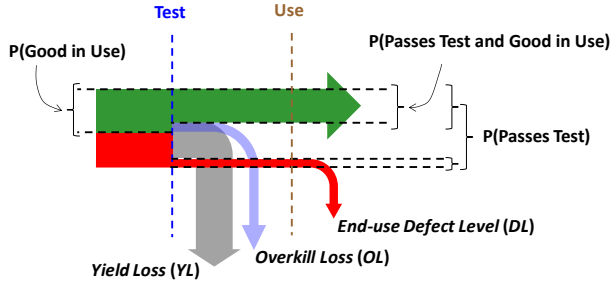


**Figure 13.** Relationship of figures of merit (*italic*) to population category probabilities.

Yield Loss given by

$$YL = P(\text{Fails Test}) = 1 - P(\text{Passes Test}) \quad (30)$$

is the fraction of manufactured arrays rejected by Test.  $YL$  is a primary manufacturing indicator since it directly affects producer costs.

Overkill Loss given by

$$OL = P(\text{Good in Use}) - P(\text{Passes Test and Good in Use}) \quad (31)$$

is the fraction of manufactured arrays (a subset of  $YL$ ) invalidly rejected by Test. Overkill affects the manufacturing cost charged to Test.

End Use Defect Level given by

$$\begin{aligned}
DL &= P(\text{Fails in Use} | \text{Passes Test}) \\
&= 1 - P(\text{Good in Use} | \text{Passes Test}) \\
&= 1 - \frac{P(\text{Passes Test and Good in Use})}{P(\text{Passes Test})} \quad (32)
\end{aligned}$$

is the customer-perceived proportion of defective arrays. It is the fraction of units classified as failing in Use, given that they have passed Test (a conditional probability).  $DL$  is a quality indicator since it affects the customer.

For business decision-making FOMs corresponding to hypothetical Test, Use (datasheet), and fault tolerance specifications are compared with targets. Only specifications meeting *all three* targets are acceptable. The FOMs defined here are designed to lie in the range  $[0,1]$  such that a larger value is less desirable. Therefore ‘‘target’’ values are regarded as the maximum acceptable values of the FOMs. Arbitrarily chosen typical targets for the product example shown below are  $YL \leq 20\%$ ,  $OL \leq 2\%$ , and  $DL \leq 200$  PPM.

Equations (2), (13), (15), (16), (17), (19), (25) or (29), (26) or (28), (27), (30), (31), and (32) provide a fully deterministic analytical model readily implemented in, say, Excel to do ‘‘what-if’’ calculations of FOMs as a function of array size, fault tolerance, Test, and datasheet (Use) specifications. The sensitivity to models of Test/Use manifestation may be explored by adjusting parameters of the transformation, Eq. (15), of the fitted copula  $C$  into the pseudo-copula  $D$  embodying these models. Since the experiment did not give the fraction of time a VRT bit is in the long retention time state, the customer-conservative assumption used in examples described next is that at Test VRT bits are in the long retention time state all of the time ( $s = 1$ ).

As an example, suppose the  $n$ -bit array has an internal mechanism, which can tolerate up to  $m$  bad bits, enabled in both Test and Use ( $m = n_u = n_t$ ). Figure 14 and Figure 15 show FOMs computed using the model for a 1 Mb ( $2^{20}$  bits) array at the maximum environmental condition of the experiment ( $V_p = 0.45$  V,  $V_d = 1.2$  V,  $T = 125^\circ\text{C}$ ) for both Test and Use, with a datasheet (Use) refresh time specification of 110 au. The FOMs are plotted as a function of the Test retention time setting which is swept past the datasheet refresh time specification (‘‘Use Condition’’).

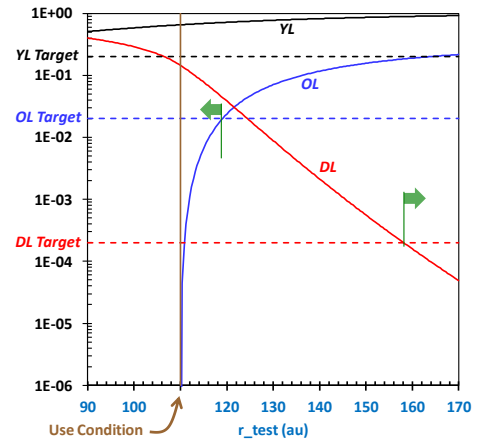


**Figure 14.** Figures of merit vs. Test retention time set point for a 1 Mb array with no fault tolerance  $m = 0$ , assuming  $s = 1$ .

There is no Test retention time setting for which all three FOM targets are met. Arrows show set point ranges which meet targets.

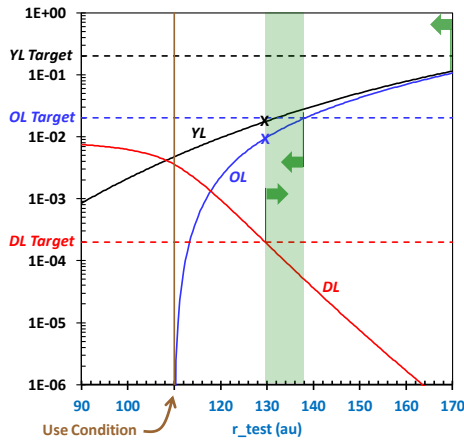


Figure 15. Figures of merit vs. Test retention time set point for a 1 Mb array which can tolerate  $m = 4$  bad bits, assuming  $s = 1$ . All FOM targets can be met for Test retention time settings between 130 and 138 au. Arrows show set point ranges which meet targets.

The design of the FOMs allows all of the FOMs to be plotted together and to be compared with their target values. Figure 14 shows that there is no setting for which a 1 Mb array with no fault tolerance ( $m = 0$ ) can meet all targets. The minimum fault tolerance capacity for which targets can all be met is  $m = 4$  bits, and Figure 15 shows this case. Notice the greatly improved yield loss in Figure 15 compared to Figure 14.

## 5. Discussion

When the rank statistics of the DRAM VRT effect is separated from complicated details of environmental dependence and shapes of marginal (Weibull) distributions an unexpected, yet simple, picture emerges. Unexpected because the usual method of fitting a bivariate normal distribution (or equivalently, Gaussian copula) cannot represent the invariance of tau under sample truncation as shown in Figure 6. Simple, because a single parameter Clayton copula with a single value for the parameter can represent this across all environmental conditions. More broadly, the DRAM case study shows the necessity of using copula methods to generalize the usual multivariate normal methods of statistical modeling of miscorrelation in semiconductor applications. The main challenge of copula methods is the need to choose a particular copula from the vast number of possibilities. For the DRAM the number of possibilities is greatly reduced because not many copulas have truncation invariance to a degree sufficient to match the data, and only the Clayton copula has complete truncation invariance.

Copula methods offer considerable practical convenience. The fitting of marginal models and copula models is decoupled, and can be done in any order. Moreover,

many copulas are well-suited to synthesizing data in limited parts of the population without rejection of Monte-Carlo-generated samples. The Clayton copula is an example of such a copula. The Gaussian copula (and therefore the multivariate normal distribution) cannot be synthesized in a limited part of the population without rejection. Rejectionless tail simulation makes Monte-Carlo simulation of the small but critical tail regions of interest in semiconductor applications highly efficient.

Key decisions at various stages of the product lifecycle require statistical models connecting device-level (bit-level for DRAM) to product-level cost and quality models. This paper provides all the machinery needed to do copula-based “what-if” analyses of effects of scaling of array size, fault tolerance (including active repair at test), datasheet (Use) specifications, and Test specifications. The statistical model may be “played forward” from bit-level to product-level to make product decisions based on computed figures of merit. But it may also be “played backwards” to discover data requirements at the device level (bit-level for DRAM) or silicon process level actually needed for product decision-making. This is important because device-level and process level characterizations can be expensive or, more significantly, time-consuming. For example, one may wish to understand the benefit of extraction of models of the RTN “duty cycle” time constants  $t_{max}$  and  $t_{min}$ . In the example of Figure 15  $s = 1$  was used as a customer-conservative assumption to determine FOMs. Figure 16 shows the effect of relaxing the assumption that Test always finds the bit in the maximum retention time state, that is, of allowing  $s$  to be less than unity. Yield loss and overkill figures of merit are shown for  $s < 1$  at test settings for which all FOMs satisfy targets. The test settings which satisfy targets all have  $DL = 200$  DPPM at the left-hand edge of the zone shown in Figure 15 as the limiting constraint.

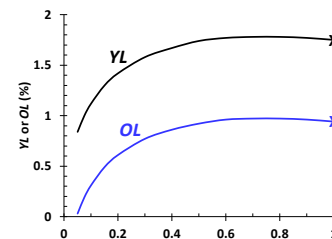


Figure 16. Yield-loss and overkill at  $DL = 200$  DPPM for the conditions of Figure 15 as a function of hypothetical VRT duty cycle,  $s$ . Values shown by X at  $s = 1$  correspond to X's in Figure 15.

Figure 16 shows that precise knowledge of  $s$  has no beneficial effect (reduction) on the overkill component of yield loss except for  $s < 0.3$ . But Kim et al [21] found values of  $s$  varying from bit-to-bit within a memory array, ranging from  $\sim 0.1$  to nearly unity. And Kim et al [8] found  $s \cong 0.55$ , weakly dependent on voltage and temperature ( $t_{max}$  and  $t_{min}$  individually depend more

strongly on temperature). Unless  $s < 0.3$  for all bits and all environmental conditions covered in Test and Use, there is no downside to setting  $s = 1$  for all model calculations. One would conclude that detailed knowledge of VRT duty cycle is probably not needed for product cost and quality decision-making for the examples of this paper.

An essential part of the method, not discussed in detail, is estimation of risks due to, a), sampling error and, b), model selection. Sampling error may be estimated using standard bootstrap methods. The semi-analytical form of the model facilitates the use of bootstrap methods [22]. When bootstrap methods are “played forward” confidence levels at which FOMs meet targets may be computed. And when “played backwards”, aspects of the design-of-experiments for bit-level data acquisition (such as sample size) required to meet targets at specific confidence levels may be determined.

Model selection risk estimation requires evaluation of FOMs using copulas of various kinds fitted to the data. The decoupling of copula models from the marginal models makes it easy to “plug in” different copulas, recompute FOMs, and thereby quantify the risk of copula selection. For the DRAM example, truncation invariance was used to select the Clayton copula. But although the Clayton copula has absolute truncation invariance, another “geometrical” copula (not shown) which had truncation invariance to a degree sufficient to fit the data nearly as well was constructed. The shape of the FOM characteristics such as Figure 14 and Figure 15 is sensitive to whether the Clayton or the geometrical copula is chosen. The Clayton copula gave the more customer-conservative (larger value of  $r_{\text{Test}}$ ) Test setting.

An often-overlooked requirement to balance producer and customer risk in integrated circuit test manufacturing is careful design of a *complete* set of FOMs and targets. Traditional fault tolerance modeling [23] assumes perfect correlation between Test and Use and focuses on only yield loss (*YL*) and sometimes the customer-perceived defectivity (*DL*). But miscorrelation introduces another degree of freedom so that the *three* FOMs (*YL*, *DL*, *OL*) discussed in this paper are needed for decision-making. It’s also useful to design FOMs to cover [0,1] and map to “good = 0 and bad = 1” for the stakeholder most interested in the FOM. The problem is more complicated but same approach works for multiple test steps.

The DRAM VRT phenomenon does not fall neatly into classical notions of “hard” and “soft” reliability mechanisms. Since VRT bits can be stuck in a state for many minutes, or even hours, VRT bit errors are “soft” as far as Test is concerned, but “hard” as far as fault tolerance in Use is concerned. VRT is soft in Test because Test, being brief, cannot detect some bits which may fail in Use. But VRT is “hard” in Use because of the unacceptable performance effect of soft data correction of bits stuck in a failing state for extended durations. The

VRT mechanism is very different from the classical [24] picture of foreign material particles causing clusters of bad bits which are either hard failures or latent reliability defects causing infant mortality that can be made to fail (permanently) and be screened by burn-in. The VRT phenomenon is also different from classical cosmic-ray soft-error mechanisms which cause only a momentary upset in Use. But the VRT mechanism is similar to RTN instabilities observed in other devices, such as SRAMs [25], [26]. Key characteristics of RTN-based mechanisms are random spatial distributions (Figure 3 and [26]) and lack of memory in normal operation. However, stress can alter the properties of defects, changing the marginal distributions [12] (reducing  $\alpha$  in our model) and increasing the miscorrelation [27] (reducing  $\theta$  in our model).

## 6. Conclusions

There are several ways to extend the method described in this paper without introducing new concepts. First, more than one Test step increases the dimensionality of the copula and the multivariate mathematical manipulations. The increased dimensionality exacerbates the “copula choice” problem. Second, the method may be extended to multiple kinds of sub-elements (instead of bits) with differing critical areas, and multiple kinds of defects. Another extension is when the marginal variables are different, including different environmental dependence, such as *Isb* and *Fmax*. Yet another extension is to replace the Poisson model in Eq. (18) by a negative binomial model to describe “large-area” wafer-to-wafer, or lot-to-lot probability density variation [28].

An extension of the method which does require new concepts is exploration of principles governing the form of copulas in the semiconductor context in order to guide copula model selection. This is important because error associated with copula model selection is hard to gauge. A hint of the conceptual framework needed is seen in the way the copula model depends on how Test and Use are manifested, Eq. (15). And, one may ask, what is behind the remarkable truncation invariance seen in the DRAM data? The history of the development of the Clayton copula may provide a clue (see [15]).

## Acknowledgements

Thanks are due to Satoshi Suzuki for acquiring the data, and to Roger Nelsen for pointing out the truncation-invariance of the Clayton copula described by Oakes. Support of this project by the Semiconductor Research Corporation under task numbers 1608.1 and 2095.1 is gratefully acknowledged.

## References

- [1] D. S. Yaney, C. Y. Lu, R. A. Kohler, M. J. Kelly, and J. T. Nelson, "A meta-stable leakage phenomenon in DRAM charge storage - variable hold time," in *International Electron Devices Meeting (IEDM)*, vol. 33, 1987, pp. 336-339. [Online]. <http://dx.doi.org/10.1109/IEDM.1987.191425>
- [2] P. J. Restle, J. W. Park, and B. F. Lloyd, "DRAM Variable Retention Time," in *International Electron Devices Meeting (IEDM)*, 1992, pp. 807-810. [Online]. <http://dx.doi.org/10.1109/IEDM.1992.307481>
- [3] Yuki Mori, Kiyonori Ohyu, Kensuke Okonogi, and Ren-ichi Yamada, "The Origin of Variable Retention Time in DRAM," in *International Electron Devices Meeting (IEDM)*, 2005, pp. 1034 - 1037. [Online]. <http://dx.doi.org/10.1109/IEDM.2005.1609541>
- [4] Yuki Mori, Hiroyuki Yoshimoto, Kenichi Takeda, and Ren-Ichi Yamada, "Mechanism of random telegraph noise in junction leakage current of metal-oxide-semiconductor field-effect transistor," *J. Appl. Phys.*, vol. 111, p. 104513, 2012. [Online]. <http://dx.doi.org/10.1063/1.4721658>
- [5] T. Umeda et al., "Single silicon vacancy-oxygen complex defect and variable retention time phenomenon in dynamic random access memories," *Applied Physics Letters*, vol. 88, p. 253504, 2006. [Online]. <http://dx.doi.org/10.1063/1.2213966>
- [6] K. Ohyu et al., "Quantitative identification for the physical origin of variable retention time: A vacancy-oxygen complex defect model," in *International Electron Devices Meeting, 2006. IEDM '06.*, 2006, pp. 1-4. [Online]. <http://dx.doi.org/10.1109/IEDM.2006.346792>
- [7] Bryan D. Boatright, Ben J. Eapen, Carvin Glenn Shirley, and Carl Scafidi, "Methods and Apparatuses for Reducing Infant Mortality in Semiconductor Devices Utilizing Static Random Access Memory (SRAM)," United States Patent Number 7197670 B2, March 27, 2007.
- [8] Heesang Kim et al., "Characterization of the Variable Retention Time in Dynamic Random Access Memory," *IEEE Transactions on Electron Devices*, vol. 58, no. 9, pp. 2952-2958, September 2011. [Online]. <http://dx.doi.org/10.1109/TED.2011.2160066>
- [9] Paul Embrechts, Alexander McNeil, and Daniel Straumann, "Correlation: Pitfalls and Alternatives," *RISK Magazine*, pp. 69-71, May 1999. [Online]. <http://www.math.ethz.ch/~baltes/ftp/papers.html>
- [10] Roger B. Nelsen, *An Introduction to Copulas*, 2nd ed. New York, New York, USA: Springer, 2010.
- [11] Pravin K. Trivedi and David M. Zimmer, "Copula Modeling: An Introduction for Practitioners," *Foundations and Trends in Econometrics*, vol. 1, no. 1, pp. 1-111, 2005. [Online]. <http://dx.doi.org/10.1561/0800000005>
- [12] Mark White, Jin Qin, and Joseph B. Bernstein, "A study of scaling effects on DRAM reliability," in *2011 Proceedings - Annual Reliability and Maintainability Symposium (RAMS)*, Lake Buena Vista, FL, 2011, pp. 1-6. [Online]. <http://dx.doi.org/10.1109/RAMS.2011.5754522>
- [13] Udo Lieneweg, Duc N. Nguyen, and Brent R. Blaes, "Assessment of DRAM Reliability from Retention Time Measurements," Jet Propulsion Laboratory, California Institute of Technology, Pasadena, Flight Readiness Technology Assessment, NASA EEE Parts Program 1998. [Online]. [http://parts.jpl.nasa.gov/cots/external/dram\\_ret.pdf](http://parts.jpl.nasa.gov/cots/external/dram_ret.pdf)
- [14] M. G. Kendall and Jean Dickinson Gibbons, *Rank Correlation Methods*, 5th ed., 1990.
- [15] David Oakes, "On the preservation of copula structure under truncation," *The Canadian Journal of Statistics*, vol. 33, no. 3, pp. 465-468, September 2005. [Online]. <http://www.jstor.org/stable/25046191?origin=JSTOR-pdf>
- [16] Alan Genz, "Numerical computation of rectangular bivariate and trivariate normal and t probabilities," *Statistics and Computing*, vol. 14, pp. 251-260, 2004. [Online]. <http://dx.doi.org/10.1023/B:STCO.0000035304.20635.31>
- [17] Margaret Armstrong, "Copula Catalogue. Part 1 : Bivariate Archimedean Copulas," CERNA - Centre d'économie industrielle, Paris, France, 2003. [Online]. <http://www.cerna.enscm.fr/Documents/MA-CopulaCatalogue.pdf>
- [18] Jorge Navarro and Fabio Spizzichino, "On the relationships between copulas of order statistics and marginal distributions," *Statistics and Probability Letters*, vol. 80, no. 5-6, pp. 473-479, March 2010. [Online]. <http://dx.doi.org/10.1016/j.spl.2009.11.025>
- [19] J. T. Campbell, "The Poisson Correlation Function," *Proceedings of the Edinburgh Mathematical Society*, vol. 4, no. 1, pp. 18-26, March 1934. [Online]. <http://dx.doi.org/10.1017/S0013091500024135>
- [20] N. L. Johnson, S. Kotz, and N. Balakrishnan, *Discrete Multivariate Distributions*. New York, N.Y.: John Wiley & Sons, Inc., 1997.
- [21] Heesang Kim et al., "RTS-like fluctuation in Gate Induced Drain Leakage current of Saddle-Fin type DRAM cell transistor," in *2009 IEEE International Electron Devices Meeting (IEDM)*, Baltimore, 2009, pp. 1-4. [Online]. <http://dx.doi.org/10.1109/IEDM.2009.5424370>

- [22] Bradley Efron and Gail Gong, "A Leisurely Look at the Bootstrap, the Jackknife, and Cross-Validation," *The American Statistician*, vol. 37, no. 1, pp. 36-48, February 1983. [Online].  
<http://www.jstor.org/stable/2685844>
- [23] Charles H. Stapper, A. N. McLaren, and M. Dreckman, "Yield Model for Productivity Optimization of VLSI Memory Chips with Redundancy and Partially Good Product," *IBM J. Res. Develop.*, vol. 24, no. 3, pp. 398-409, May 1980.
- [24] Charles H. Stapper, "Correlation analysis of particle clusters on integrated circuit wafers," *IBM J. Res. Develop.*, vol. 31, no. 6, pp. 641-650, November 1987.
- [25] Marty Agostinelli et al., "Erratic Fluctuations of SRAM Cache Vmin at the 90nm Process Technology Node," in *IEDM Technical Digest, IEEE International Electron Devices Meeting*, Washington, D.C., 2005, pp. 655-658. [Online].  
<http://dx.doi.org/10.1109/IEDM.2005.1609436>
- [26] K. Takeuchi et al., "Direct observation of RTN-induced SRAM failure by accelerated testing and its application to product reliability assessment," in *2010 Symposium on VLSI Technology (VLSIT)*, Honolulu, HI, 2010, pp. 189-190. [Online].  
<http://dx.doi.org/10.1109/VLSIT.2010.5556222>
- [27] Y. I. Kim, K. H. Yang, and W. S. Lee, "Thermal degradation of DRAM retention time: Characterization and improving techniques," in *2004 IEEE International Reliability Physics Symposium Proceedings*, 2004, pp. 667-668. [Online].  
<http://dx.doi.org/10.1109/RELPHY.2004.1315442>
- [28] Charles H. Stapper, "Large area fault-clusters and fault tolerance in VLSI circuits: A review," *IBM J. Res. Develop.*, vol. 33, no. 2, pp. 162-172, March 1989.